Electric-current distortion effects in polycystalline copper†

P. M. Martin,* J. B. Sampsell, and J. C. Garland
Department of Physics, The Ohio State University, Columbus, Ohio 43210
(Received 27 September 1976)

Unusual electric-current distortion effects are known to occur in materials having a conductivity tensor which is both anisotropic and spatially inhomogeneous. Both of these conditions are satisfied in strong magnetic fields by polycrystalline noble metals. This paper reports on a comprehensive study of the galvanomagnetic properties of polycrystalline copper at liquid-helium temperatures. A flat plate geometry was used which made it possible to distinguish current distortion effects from intrinsic, band-structure-related effects. In addition to summarizing the results of transverse and longitudinal magnetoresistance and Hall-effect measurements on 20 specimens, model calculations of the current flow pattern around isolated crystallites containing open orbits are also given.

I. INTRODUCTION

The electric current distribution in an inhomogeneous medium having a scalar conductivity $\sigma(\vec{r})$ is in principle quite obvious; in accordance with Ohm's law the current density becomes concentrated in regions of high conductivity while avoiding regions of low conductivity. The effective conductivity of the medium is equal to a straightforward volume average of the local conductivity. On the other hand, if an inhomogeneous medium has an anisotropic conductivity, described by a tensor $\bar{\sigma}(\vec{r})$, then the transport properties of the medium cannot be so easily determined. The electrostatic potential does not in general satisfy Laplace's equation and the effective conductivity is not conveniently equal to the average conductivity. The electric current in such systems may even flow along intuitively unexpected trajectories, for example, avoiding high-conductivity regions in favor of regions where the diagonal conductivity is low.

There are many systems under investigation which exhibit the effects of inhomogeneities. Unusual galvanomagnetic effects in crystalline semiconductors are known to result from macroscopic inhomogeneities arising from crystal imperfections, bonding defects, impurity clusters, or uneven concentrations of doping elements.[1] Anomalies in the galvanomagnetic properties of disordered systems such as the chalcogenide glasses[2] are also thought to result from the presence of inhomogeneities, and such anomalies can also occur in materials which undergo metal-semiconductor transitions such as expanded liquid mercury,[3-5] liquid tellurium,[6,7] and metal-ammonia compounds.[7,8] Current distortion effects in charge transfer salts have been suggested as a partial explanation of some unusual temperature-dependent conductivity measurements reported by several workers.[9]

As a final example we consider the unusual galvanomagnetic behavior of the free-electron metals, specifically the linear magnetoresistance frequently observed in samples of potassium, sodium, aluminum, and indium.[10-15] Recent calculations by Sampsell and Garland,[16] and Stroud and Pan,[17] of the galvanomagnetic properties of a free-electron medium containing isolated nonconducting inclusions have shown that current distortions can propagate along directions parallel to the magnetic field for distances of order $\omega_c \tau D$, where ω_c is the cyclotron frequency, τ is the relaxation time, and D is the characteristic size of the inclusions. The excess concentration of current in the distorted regions leads to a high-field magnetoresistance which is a linear function of magnetic field.

A polycrystalline noble metal is in several respects an ideal system for studying current distortion effects of the type just described. A variety of orbit types are possible in a magnetic field, including strictly closed orbits, extended orbits, and single and double open orbits.[18] If the orientations of crystallites are randomly distributed, about 90% of the crystallites will support only closed orbits and will have a conductivity tensor which is very nearly that of an ideal free-electron metal. These closed-orbit crystallites may thus be thought of as comprising a free-electron background medium within which may be found isolated regions having a conductivity characteristic of open or extended orbits. Current injected uniformly into this medium will thus encounter regions where the local conductivity changes discontinuously, and the resulting redistribution of the lines of electric current near these discontinuities will produce an excess joule dissipation and consequent magnetoresistance. The explicit field dependence of the magnetoresistance will depend on the allowed electron orbits in the "singular" crys-

tallites, the detailed geometry of the crystallites, and any interaction between distortion fields from neighboring singular crystallites.

Although the essential galvanomagnetic properties of polycrystalline copper were established in 1929 by Kapitza,[19] the subject received little theoretical attention until 1958 when Ziman[20] calculated a general conductivity tensor for copper. The magnetoconductivity of polycrystalline copper was computed from an angular average of this conductivity tensor over all possible orientations; this procedure, which ignored current distortion effects, yielded a linear transverse and longitudinal magnetoresistance and a field-independent Hall coefficient about 60% as large as the free-electron value. A statistical model for the transport properties of inhomogeneous conductors has been developed by Herring[21] using second-order perturbation theory. The model is applicable to the weak magnetic field limit of polycrystalline copper, and predicts a quadratic field dependence for the low-field transverse and longitudinal magnetoresistance. Bruggeman,[22] Landauer,[23] Stachowiak,[24] Schotte and Jacob,[25] and Stroud[26] have developed self-consistent effective medium approaches to the problem which are not restricted to weakly varying conductivities. According to the Stachowiak model open orbits are found to lead to a saturating transverse magnetoresistance, while extended orbits in the absence of small-angle scattering generate an $(\omega_c\tau)^{2/3}$ field dependence. If the incidence of small-angle scattering is great enough, the transverse magnetoresistance is found to exhibit a prolonged linear growth. The influence of extended orbits has also been studied by Dreizen and Dykhne[27] who derived an expression for the high-field conductivity of a polycrystalline noble metal which is in accord with the calculations of Stachowiak.

There are few explicit calculations of the current distortion pattern around crystallites containing open or extended orbits. Herring[21] has discussed the qualitative features of current flow around an isolated cylindrical inclusion having an arbitrary conductivity, and Sampsell and Garland[16] have obtained exact expressions for the current flow around isolated cylindrical and spherical voids in a free-electron metal. Interactions between nonisolated inhomogeneities have recently received attention by Dreizen and Dykhne,[28] who have proposed an interesting qualitative model for current flow in polycrystals. According to their model, in a strong magnetic field the preponderance of crystallites have a conductivity which is essentially one dimensional and aligned along the direction of the magnetic field. Occasional singular crystallites have a significant open or extended orbit conductivity which is transverse to the field. A transverse current will thus be able to work its way across the polycrystal by following a network in which the singular crystallites are linked together by the large longitudinal conductivity of the background medium. If the dimension of the sample parallel to the magnetic field direction d is smaller than a critical value d_0, the current path will be broken and the effective magnetoconductivity of the polycrystal will drop. This size effect has not been verified experimentally.

There are a large number of experimental studies of the galvanomagnetic properties of copper although few of them have been specifically concerned with polycrystalline samples. Interested readers should refer to the comprehensive bibliography prepared by Fickett.[29] Kapitza[19] performed the first well-known magnetoresistance experiments on polycrystalline copper in 1929. He found that in weak magnetic fields ($\omega_c\tau \ll 1$) the transverse magnetoresistance varied quadratically, while in strong fields ($\omega_c\tau \gg 1$) it increased as a linear function of magnetic field. These conclusions have been generally corroborated by other workers, most recently by Fickett[29,30] in a comprehensive study of the transverse magnetoresistance of eight polycrystalline copper wires. Fickett determined that the magnetoresistance of all the specimens studied could be described by a universal curve on a Kohler magnetoresistance diagram. Data for all samples could be adequately represented by an expression of the form

$$\ln[\rho(\omega_c\tau)-\rho(0)]/\rho(0) = A_0 + A_1 \ln\omega_c\tau + A_2(\ln\omega_c\tau)^2 . \quad (1)$$

In spite of these results, Kohler's rule is not invariably found to be obeyed in copper, deviations having been attributed to magnetic impurities,[31] the onset of electron-phonon scattering at high temperatures,[32] small-angle scattering,[33,34] or boundary scattering.[35] In impurity dominated wire samples, however, it appears that the magnetoresistance of polycrystalline copper is in close accord with Kohler's rule as long as the diameter of the wire is significantly larger than the average size of the crystallites.

In this paper we report on measurements of the longitudinal and transverse magnetoresistance and Hall effect of 20 polycrystalline copper samples at liquid-helium temperatures. A flat plate geometry was used in order to differentiate long-range current distortion effects from other possible causes of the linear magnetoresistance. The galvanomagnetic properties of single crystalline copper were also studied with particular emphasis on the magnetic field dependence of the transverse

magnetoresistance for closed-orbit and extended-orbit crystal orientations. In the Appendix, the current distribution around isolated cylindrical crystallites containing open orbits is calculated, and computer generated drawings of the current flow pattern are used to interpret the experimental results. A detailed effective medium theory of the magnetoresistance of polycrystalline copper for our geometry will be published by Pan and Stroud.

II. EXPERIMENTAL DETAILS

A. Sample preparation

The polycrystalline copper ingots used in this experiment were supplied by the American Smelting and Refining Co. (Asarco), Cominco, Inc., and Atomergic Chemetals Co., and were nominally 99.999% pure. Single-crystal copper stock was obtained from the Materials Research Corp. (MRC). Polycrystalline samples cut directly from the supplier's ingots had reasonably uniform crystallite sizes, ranging from 0.02 cm in diameter for Cominco copper, to 0.07 cm for Asarco copper. The residual resistance ratio $\rho(290\ \mathrm{K})/\rho(4.2\ \mathrm{K})$ of the starting material varied from 50 to about 600. Samples were cut to size with a spark-erosion cutter and then etched in dilute HNO_3 to remove surface damage. Each sample was then examined under a traveling microscope so that the size and distribution of crystallites could be determined. The orientations of single-crystal samples were verified by x-ray analysis.

In order to increase the range of electrical purities available for investigation, most samples were annealed for 3 h at a temperature of $960 \pm 5\,^{\circ}\mathrm{C}$ in an oxygen atmosphere of pressure 2×10^{-4} Torr. After annealing, sample residual resistance ratios ranged from about 1200 to 10 000 for polycrystalline specimens and to about 20 000 for single-crystal samples. The average grain size of the polycrystalline samples was generally observed to increase after annealing, occasionally by as much as 50%. The physical dimensions, average grain size, and residual resistivity ratio of all the polycrystalline copper samples are summarized in Table I.

TABLE I. Physical characteristics of copper samples.

Sample No.[a]	Supplier	$\frac{\rho(273)}{\rho(2.4)}$	Thickness (cm)	Length (cm)	Width (cm)	r_g[b] (cm)
2A	Cominco	272	0.078	2.512	0.934	0.039
3	Cominco	388	0.055	2.518	0.952	0.059
3A	Cominco	1353	0.055	2.518	0.952	0.036
4A	Asarco	1709	0.055	1.859	0.777	0.100
5	Asarco	667	0.073	2.541	0.964	0.096
6A	Asarco	8890	0.055	2.503	0.978	0.133
7A	Atom. Chem.	8670	0.058	2.553	0.951	0.062
7AA	Atom. Chem.	9820	0.058	1.868	0.748	0.052
8A	Asarco	6290	0.076	2.510	0.959	0.055
8AA[d]	Asarco	2840	0.076	1.838	0.783	0.061
9A	Cominco	1975	0.061	2.535	0.960	0.030
9AA	Cominco	3420	0.061	1.862	0.738	0.030
10A	Asarco	8190	0.064	2.512	0.962	0.107
11A	Atom. Chem.	4190	0.027	2.520	0.938	0.109
12A	Atom. Chem.	3690	0.031	2.519	0.947	0.194
13A	Atom. Chem.	1930	0.031	1.846	0.790	0.092
15A	Cominco	10 040	0.018	2.507	0.953	0.349
17A	Cominco	2031	0.037	2.515	0.947	0.027
18A	Atom. Chem.	6830	0.053	1.868	0.748	0.051
20[c]	MRC	1740	0.204	1.866	0.262	...
20S[c]	MRC	5470	0.204	1.866	0.262	...
20A[c]	MRC	20 100	0.204	1.866	0.262	...

[a] The suffix *A* following the designation number means the sample was annealed in an oxidizing atmosphere, as described in the text. The suffix *AA* means the sample was annealed twice on separate occasions. The suffix *S* refers to strain relief annealing in a vacuum at 500 °C.

[b] Average crystallite diameter. Typically crystallite diameters (d_c) for a given sample ranged over approximately an order of magnitude from $4r_g < d_{c\max} < 6r_g$ to $\frac{1}{4}r_g < d_{c\min} < \frac{1}{2}r_g$.

[c] Single crystal.

[d] Sample was unintentionally contaminated with excessive oxygen during the second annealing treatment.

B. dc magnetoresistance and Hall-effect measurements

All dc measurements were made by a four-probe method using the instrumentation shown in Fig. 1(a). Currents of 1–5 A were supplied to the sample by a Kepco BOP-36-5(M) operational amplifier operated in a constant-current mode, and the potential developed between the voltage leads was measured by either a Keithley 140 dc amplifier or a Keithley 148 nanovoltmeter. The amplified voltage was monitored simultaneously on an x-y recorder and a digital voltmeter. A maximum magnetic field of 7.5 T was available from a superconducting solenoid; field measurements are believed accurate to at least 0.1% and are traceable to NMR calibration.

Because of the importance of insuring a uniform current injection into the samples and avoiding undesirable electrode effects, particular care was taken in the design of current and voltage electrodes [see the inset in Fig. 1(a)]. The voltage electrodes were made of tiny brass pins mounted in a phenolic holder. Brass bearings in the holder permitted the pins to slide freely while maintaining a uniform spacing. Phospher bronze coil springs pressed the pointed ends of the pins against the sample. The current electrodes were made of brass and were cemented to the ends of the samples with Acheson Electrodag No. 413 silver paste. In order to assure proper electrode alignment, the sample, current electrodes, and voltage electrodes were assembled together in an alignment fixture which positioned the electrodes correctly while the silver paste solidified. After solidification, the sample and electrode assembly was mounted as a unit in the sample rotator which was then positioned inside the superconducting solenoid. The rotator was motor driven and permitted all possible orientations of the sample to be achieved. Because of this feature, rotation diagrams of the transverse magnetoresistance as well as measurements of longitudinal magnetoresistance could be made without removing the specimen from the liquid-helium bath.

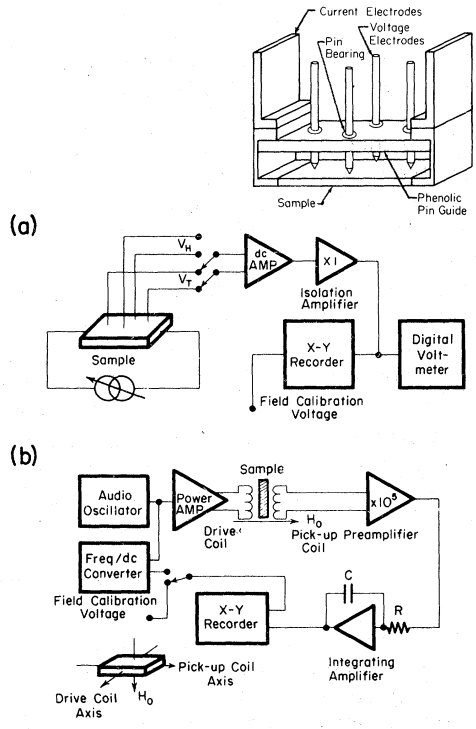

FIG. 1. (a) Diagram of the instrumentation used in dc magnetoresistance and Hall-effect measurements. The inset shows the electrode configuration. (b) Diagram of the instrumentation used in the standing-wave helicon magnetoresistance measurements.

C. Standing-wave helicon measurements

The transverse magnetoresistance and Hall coefficient of several polycrystalline samples were studied by means of the standing-wave helicon technique in order to see whether the results obtained by inductive measurements were consistent with those from four-probe dc measurements. Rectangular flat plate samples were used, and in all cases the magnetic field was oriented perpendicular to the large face of the plate. The instrumentation used in the helicon measurements is shown in Fig. 1(b). Helicon waves could be excited in the samples over the frequency range 25 Hz–10 kHz by Helmholtz coils driven by a function generator and power amplifier. The voltage induced in the pickup coil was amplified, integrated to remove a factor of frequency, detected, and applied to the Y input of an x-y recorder. At the same time, a voltage proportional to either the excitation frequency or the magnetic field strength was applied to the X input of the recorder so that the resulting trace corresponded to the modulus of the standing-wave resonance. Because signal voltages were typically 10^{-5}–10^{-3} V at high fields it was not necessary to use phase sensitive detection to obtain good signal-to-noise ratios.

A comprehensive analysis of the standing-wave helicon resonance for the rectangular plate geometry has been given elsewhere.[36] The appropriate expressions for the transverse magnetoresistance $\rho(B_0)$ and Hall coefficient R in terms of the standing-wave resonance parameters are

$$f_r = kRB_0(1+1/u^2)^{1/2}, \quad u \propto V_p . \tag{2}$$

Here f_r is the helicon resonance frequency, V_p is the rms signal voltage at resoance, $u = RB_0/\rho(B)$

is the tangent of the Hall angle, and the coefficient k is a geometry factor characteristic of the particular sample dimensions. It can be shown that u is related to the Q of the resonance by $u = (4Q^2 - 1)^{1/2}$, so that the transverse magnetoresistance and Hall coefficient can be determined from measurements of f_r, V_p, and Q.

III. EXPERIMENTAL RESULTS

A. Single crystalline copper

While this work was primarily concerned with polycrystalline copper, we felt it important to obtain measurements of the field dependence of the magnetoresistance for specific closed-orbit and extended-orbit crystal orientations in order to determine the suitability of the model conductivity tensor used in our analysis. We were also particularly interested in possible departures from Kohler's rule in single-crystal material since such departures had been observed for some of our polycrystalline samples. Figure 2(a) shows a [111] projection of the copper Fermi surface showing open and closed-orbit directions for transverse fields, as determined by Klauder *et al.*[37] The current direction for sample 20 is shown in the figure and is seen to be transverse to the [111] direction, and about 7° from the [112] direction. A rotation diagram for the transverse magnetoresistance is obtained by sweeping the magnetic field along the great circle trajectory shown as the dashed line in the figure. Shaded areas correspond to regions having an open-orbit (quadratic) magnetoresistance; lines radiating away from shaded regions indicate the presence of one-dimensional open orbits.

Figure 2(b) shows a magnetoresistance rotation diagram at $B = 5.9$ T for sample 20 in an unannealed

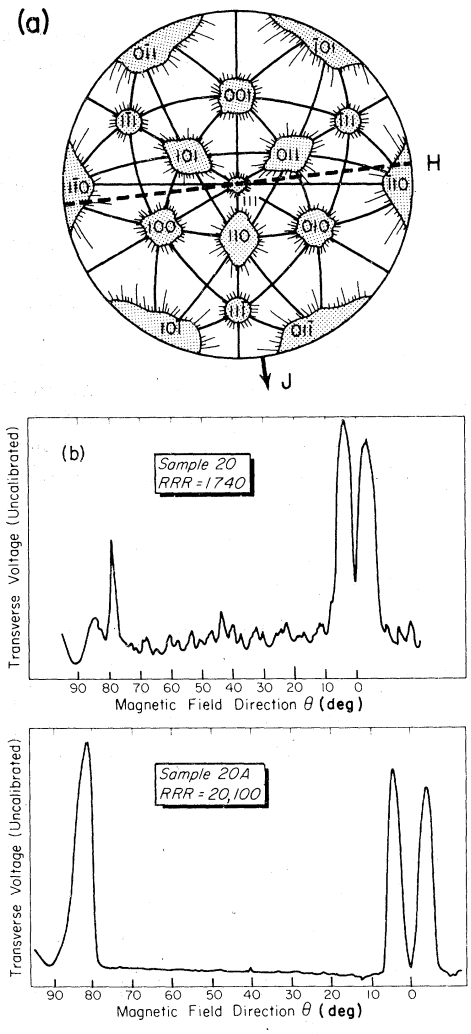

FIG. 2. (a) Stereographic projection of the Fermi surface of copper, centered on the [111] direction after Klauder *et al.* Shaded regions have a quadratic magnetoresistance. The current and magnetic field directions for sample 20 are shown on the projection. (b) Rotation diagram of the transverse magnetoresistance of samples 20 and 20A at $B = 5.9$ T. The residual resistance ratio (RRR) of each sample is given.

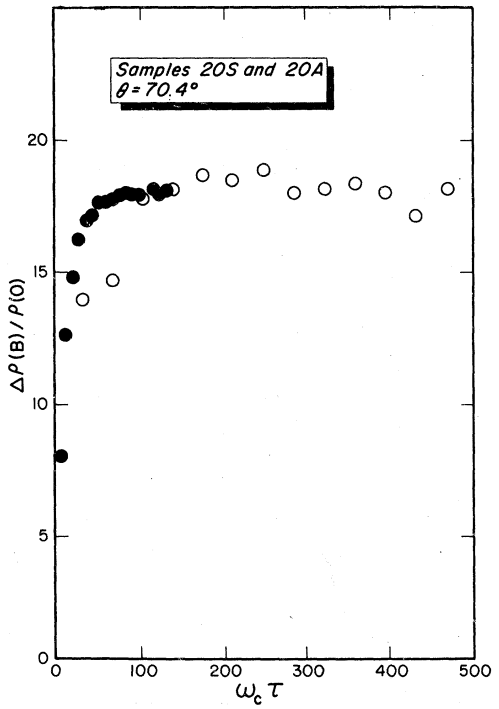

FIG. 3. Transverse magnetoresistance of samples 20*S* (closed circles) and 20*A* (open circles) at $\theta = 70.4°$ illustrating high-field saturation and agreement with Kohler's rule for closed-orbit crystal orientation. For this figure, and all others, $\omega_c \tau$ was computed according to $\omega_c \tau = 4.0 \times 10^{-3}$ [RRR times B_0 (T)].

(20) and annealed state (20A). The large peaks in the magnetoresistance exhibit the expected quadratic field dependence. In Fig. 3, a Kohler plot of the transverse magnetoresistance of sample 20 and 20A is shown for a representative closed-orbit orientation with a field direction of $\theta = 70.4°$. The data exhibit a convincing saturation at $\Delta\rho/\rho(0) = 18$ and show excellent agreement with Kohler's rule. A few orientations were found which appeared to have a nearly linear field dependence. An example of one of these orientations is shown in Fig. 4 for $\theta = 40.1°$, which corresponds to the location of the small peak in the rotation diagram. The slight deviation from Kohler's rule at this orientation is quite likely a result of a small alignment error which occured when sample 20 was remounted after annealing. The longitudinal magnetoresistance of sample 20, shown in Fig. 5, saturates at $\Delta\rho/\rho(0) = 1.5$.

B. Polycrystalline copper

Measurements on polycrystalline flat plate samples were made in magnetic fields up to 6.8 T. Our primary interest was in obtaining comparative measurements for the two sample orientations, designated $H_\perp$ and $H_\parallel$, shown in Fig. 6.

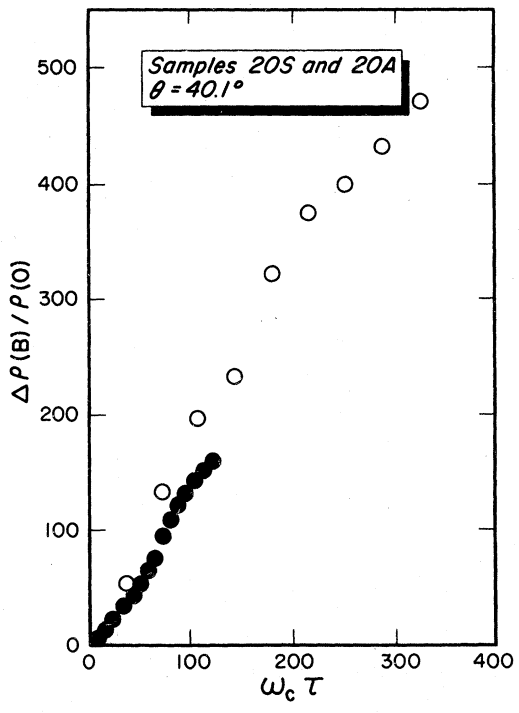

FIG. 4. Transverse magnetoresistance of sample 20S (closed circles) and 20A (open circles) at $\theta = 40.1°$ showing the intrinsic linear field dependence observed at isolated crystal orientations.

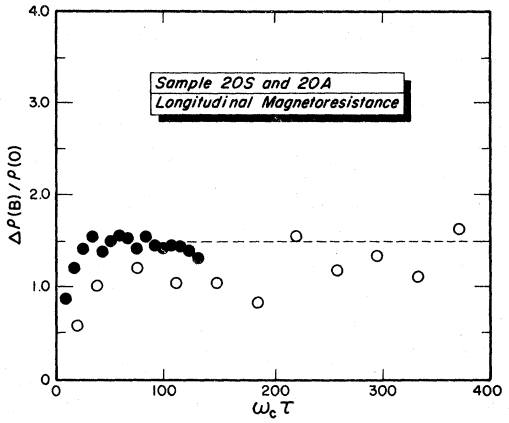

FIG. 5. Longitudinal magnetoresistance of sample 20S (closed circles) and 20A (open circles) illustrating high-field saturation and agreement with Kohler's rule.

Measurements taken at intermediate orientations were used primarily to check for spurious electrode effects. Figure 7 shows data for the $H_\perp$ and $H_\parallel$ orientations for two specimens. In Fig. 7(a), the transverse magnetoresistance of the $H_\parallel$ orientation for sample 6A is seen to increase as a linear function of magnetic field throughout the high-field regime, while magnetoresistance of the $H_\perp$ orientation shows a substantially smaller increase, apparently tending toward saturation at very strong fields. These data are representative of measurements taken on 20 polycrystalline spec-

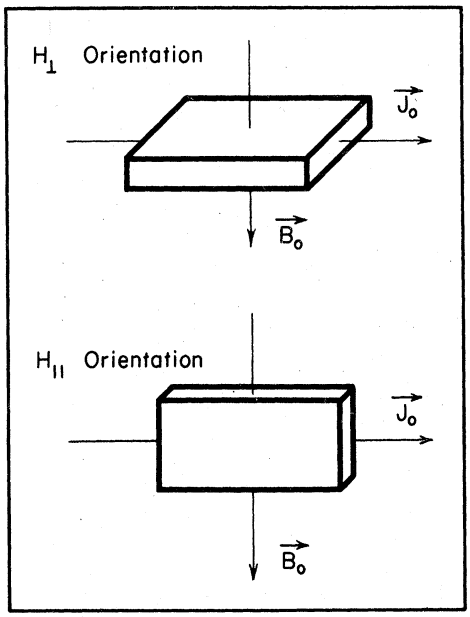

FIG. 6. Description of the $H_\perp$ and $H_\parallel$ sample orientation used in magnetoresistance measurements of polycrystalline samples.

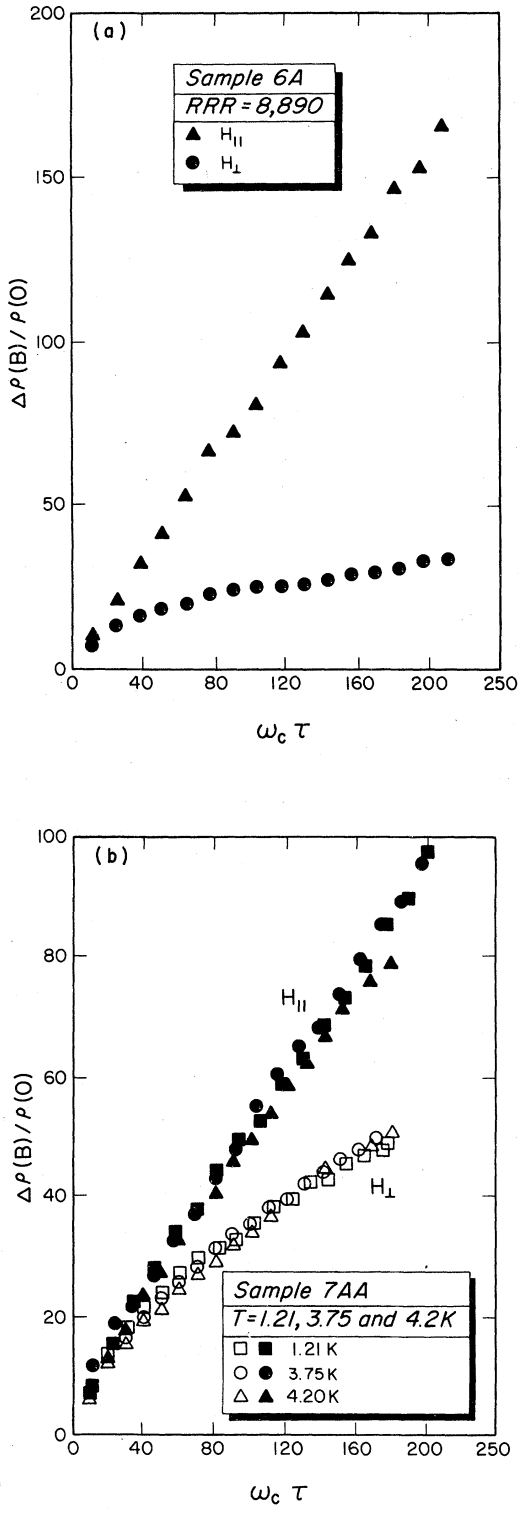

FIG. 7. (a) Transverse magnetoresistance of sample 6*A* for the $H_\perp$ and $H_\parallel$ orientation. (b) Transverse magnetoresistance of sample 7*AA* for the $H_\perp$ and $H_\parallel$ orientation at 1.21 K (squares), 3.75 K (circles), and 4.2 K (triangles).

imens. While there were appreciable sample-to-sample differences in the magnitude of the magnetoresistance, for any given sample the $H_\parallel$ orientation always had a stronger field dependence (generally linear) than the $H_\perp$ configuration. There was no discernible temperature dependence to any measurements over the limited temperature range accessible in the experiment; Fig. 7(b) illustrates this point for sample 7*AA* with data taken at 1.21, 3.75, and 4.2 K. All remaining data were obtained at 4.2 K.

In Fig. 8, Kohler plots of the transverse magnetoresistance for seven polycrystalline samples are shown for the $H_\parallel$ orientation. For each sample the magnetoresistance shows a strong nonsaturating component with, for $\omega_c\tau \gg 1$, a very nearly linear field dependence. The Kohler slope $S_\parallel$ is defined by $S_\parallel = \delta(\Delta\rho/\rho)/\delta(\omega_c\tau)$ and for these specimens varied between 0.29 and 0.84. With the exception of sample 6*A*, the field dependence of all samples at large $\omega_c\tau$ was similar. Sample 6*A* had the largest crystallite size and the largest residual resistance ratio of any of the polycrystalline samples studied. Magnetoresistance data for the same specimens are shown in Fig. 9 for the $H_\perp$ field configuration. For this configuration, the Kohler slope $S_\perp$ at large $\omega_c\tau$ varied between approximately zero for samples 12*A* and 15*A* to about 0.25 for samples 3*A*, 9*A*, 17*A*, and 8*AA*. There appeared to be a general correlation between $S_\perp$ and the dimensionless parameter $\alpha = d/r_g$ for these samples, where d is the sample thickness (measured parallel to the magnetic field in the $H_\perp$ configura-

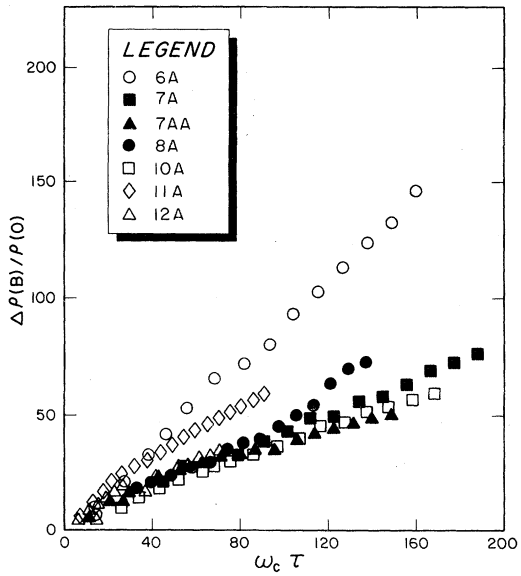

FIG. 8. Transverse magnetoresistance of seven polycrystalline samples in the $H_\perp$ orientation.

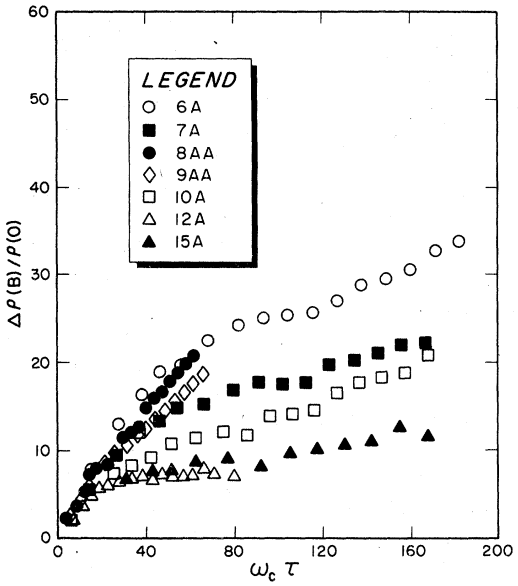

FIG. 9. Transverse magnetoresistance of seven polycrystalline samples in the $H_{\parallel}$ orientation.

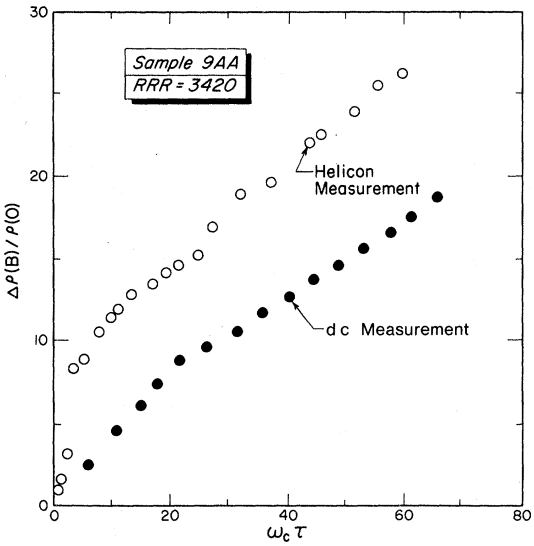

FIG. 11. Comparison of magnetoresistance data obtained by the four-probe dc method and the standing-wave helicon method for sample 9*AA* in the $H_{\perp}$ orientation.

tion) and r_g is the average crystallite grain size. The coefficient α is a measure of the extent to which crystallites extend through the sample dimension parallel to the magnetic field. For $\alpha \gg 1$, very few crystallites extend entirely through the thickness of the sample, and $S_{\perp}$ and $S_{\parallel}$ would be expected to be about equal. The relationship between $S_{\perp}$ and α is shown in Fig. 10 for 20 specimens. It should be noted that a saturating magnetoresistance is most likely to be observed when $\alpha \ll 1$, and that the wide variations in $S_{\perp}$ for neighboring values of α are not consistent with a systematic sample size effect.

Figure 11 shows transverse magnetoresistance data for sample 9*AA* obtained by the standing-wave helicon method and by the conventional dc method. Although the uncertainty in the helicon measurements is rather large because of the difficulty of determining accurately the resonance parameters, the Kohler slopes $S_{\perp}$ for the two curves agree to within 5%. Helicon measurements were also obtained for samples 7*AA* and 8*AA*, and in each case the results were compatible with those obtained using dc techniques.

In Fig. 12, the longitudinal magnetoresistance of sample 12*AA* is shown and is seen to saturate in strong fields at $\Delta\rho/\rho(0) = 2.5$. Longitudinal magnetoresistance measurements were also obtained for samples 6*AA*, 7*AA*, 8*AA*, and 9*AA*, and in each case saturation was observed at large $\omega_c\tau$.

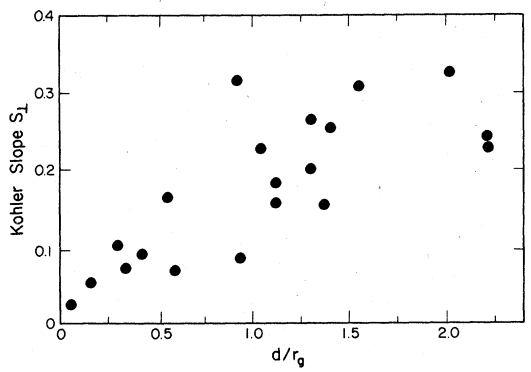

FIG. 10. Dependence of the Kohler slope $S_{\perp}$ of 20 polycrystalline samples on the parameter $\alpha = d/r_g$. All data are shown for the $H_{\perp}$ orientation.

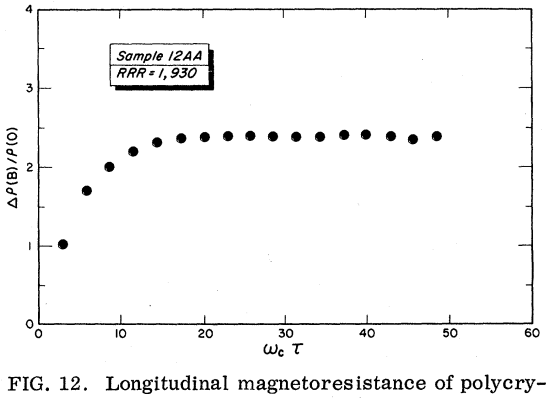

FIG. 12. Longitudinal magnetoresistance of polycrystalline sample 12*AA*, illustrating a high-field saturation at $\Delta\rho(B)/\rho(0) = 2.5$. The longitudinal magnetoresistance of all polycrystalline samples exhibited similar behavior

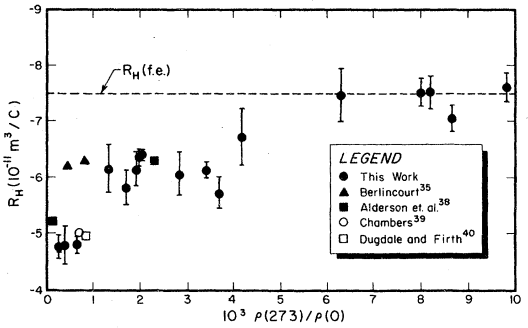

FIG. 13. Dependence of the Hall coefficient R_H on residual resistance ratio $\rho(273)/\rho(0)$ for 17 polycrystalline copper samples. Also shown for purposes of comparison are measurements by other workers. The free-electron value of R_H is shown as the dashed line in the figure.

The saturation value of $\Delta\rho/\rho(0)$ varied between 1.6 and 3.0 but did not appear to be directly correlated with either the residual resistance ratio of the specimen or the average crystallite grain size.

During the course of our measurements we determined the high-field Hall coefficients R_H of 19 polycrystalline copper samples. As expected, R_H for each sample was found to be independent of magnetic field strength. However, we did observe a surprising dependence of R_H on sample residual resistivity ratio. This dependence is illustrated in Fig. 13 where, for purposes of comparison, values of R_H observed by Alderson *et al.*,[38] Berlincourt,[35] Chambers,[39] and Dugdale and Firth[40] are also shown, It is reasonable to conclude from the figure that the Hall coefficient in very pure polycrystalline copper is very nearly equal to the free-electron value of 7.5×10^{-11} m^3/C. Table I provides a summary of the data on our different samples.

TABLE II. Summary of polycrystalline copper data.

Sample No.	$S_\perp$ [a]	$S_\parallel$ [a]	$-R_H$ (10^{-11} m^3/C)	LMR [b] saturation	$\alpha = \frac{d}{r_g}$
2A	0.753	•••	4.76	•••	1.99
3	0.315	•••	4.79	•••	0.92
3A	0.305	0.365	6.14	•••	1.54
4A	0.163	0.470	5.80	1.97	0.55
5	•••	•••	4.80	•••	0.76
6A	0.092	0.835	•••	•••	0.41
7A	0.084	0.355	7.02	•••	0.94
7AA	0.155	0.295	7.58	2.92	1.12
7AA [c]	0.182	•••	•••	•••	1.12
8A	0.152	0.470	7.44	•••	1.38
8AA	0.265	0.378	6.03	1.60	1.25
8AA [c]	0.200	•••	•••	•••	•••
9A	0.325	0.438	6.33	•••	2.03
9AA	0.228	0.275	6.11	2.88	2.03
10A	0.070	0.308	7.50	•••	0.60
11A	0.103	0.495	6.70	•••	0.25
12A	0.030	0.340	5.71	•••	0.16
13A	0.074	0.365	6.13	2.40	0.34
15A	0.026	•••	•••	•••	0.05
17A	0.253	0.368	6.39	•••	1.37
18A	0.227	0.470	7.49	•••	1.04

[a] Kohler slope S defined by $S \equiv \delta(\Delta\rho/\rho_0)/\delta\omega_c\tau$.

[b] Saturation value of the longitudinal magnetoresistance (LMR) $\Delta\rho/\rho_0$ at large $\omega_c\tau$.

[c] Measured by helicon method.

IV. DISCUSSION

A comprehensive theory of the magnetoresistance of polycrystalline copper for the geometries studied in this work will be reported by Stroud and Pan, using the effective medium approximation. In this section, we are primarily concerned with the general features of the long-range distortions of the electric current distribution brought on by intrinsic conductivity fluctuations. For purposes of comparison we first consider some features of the magnetoresistance of high-purity single crystals of copper.

Both the transverse and longitudinal magnetoresistance of all of our single-crystal specimens showed a strict saturation at large $\omega_c\tau$ for closed orbit field orientations. Although predicted by Lifshitz, Azbel, and Kaganov,[41] saturation has in fact seldom been observed in the simple nearly-free-electron metals. We believe the absence of the linear term in the closed-orbit magnetoresistance of copper to be quite surprising, therefore, and conclude that copper is one of the few metals whose magnetoresistance seems to be generally in accord with the basic predictions of the Lifshitz-Azbel-Kaganov theory.

There are a few isolated crystal orientations of copper in which a linear transverse magnetoresistance appears to result from intrinsic band structure effects. The data shown in Fig. 4 illustrates this point. It should be noted that the linear term does not occur at the interface between closed-orbit and open-orbit regions of the Fermi surface, where the transition between a saturating and quadratic magnetoresistance might be expected to produce a quasilinear field dependence. We are aware of no electron orbit configuration which could produce this observed linear field dependence. However, these anomalous regions appear to comprise such a small part of the copper Fermi surface that we believe their contribution may be reasonably neglected in the analysis of the composite magnetoresistance of our polycrystalline samples.

As discussed in Sec. III, our study of the mag-

netoresistance of polycrystalline copper concentrates primarily on thin flat plate samples. In this geometry, current distortion effects are evident as a rotation anisotropy in the transverse magnetoresistance at large $\omega_c\tau$. The current distortions and the resulting magnetoresistance are expected to be most pronounced in the $H_{\parallel}$ orientation where the sample dimension parallel to the magnetic field is much larger than the mean crystalline diameter. Because of the intrinsic two-dimensional character of the flat plate geometry, the distortion-induced magnetoresistance of this configuration is not comparable to the magnetoresistance of cylindrical polycrystalline wires. Even so, a comparison of our data with the polycrystalline wire data of Fickett[29,30] reveals a rough correspondence in the coefficients of the linear magnetoresistance. The principal difference between the wire geometry and the flat plate geometry appears to lie in substantial deviations from Kohler's rule which were observed in the latter. These deviations took the form of sample-to-sample variations in the Kohler slope and did not appear to be associated with the residual resistance ratio, annealing history, or crystallite size of the samples. We believe these departures from Kohler's rule are most likely a consequence of the imperfect statistics of our polycrystalline samples. The number of crystallites in some samples, particularly 12A and 15A, was probably not great enough to insure a random statistical distribution, thus leading to a "sampling error" in the data for the composite mixture.

In order to illuminate some general features of the current distortion effects in the $H_{\parallel}$ field configuration, we have carried out calculations of the electric current distribution around isolated singular crystallites. In our model, details of which are given in the Appendix, we consider a free-electron background medium containing a single open-orbit crystallite. The crystallite is assumed to be an infinitely long cylinder whose axis is perpendicular to both the magnetic field and the direction of current injection. We assume that the crystallite has a single open-orbit channel which lies in a plane normal to the magnetic field and which is inclined at an angle θ away from the current direction. The conductivity tensor for this crystallite has components

$$\begin{aligned}
\sigma_{11} &= \sigma_0[(1-f)\gamma + f\cos^2\theta], \\
\sigma_{22} &= \sigma_0[(1-f)\gamma + f\sin^2\theta], \\
\sigma_{12} &= \sigma_0[(1-f)\beta\gamma + f\sin\theta\cos\theta], \\
\sigma_{21} &= \sigma_0[-(1-f)\beta\gamma + f\sin\theta\cos\theta].
\end{aligned} \tag{3}$$

In the above expressions $\beta = \omega_c\tau$, $\gamma = (1+\beta^2)^{-1}$, and f is the "strength" of the open-orbit channel which may be taken to be approximately equal to the fraction of the Fermi surface area given to open-orbit conduction. In the ensuing discussion we have chosen $f = 0.1$ to be representative of open orbits in copper.

Figure 14 shows the projection on the x-z plane of the electric current distribution near an open-orbit crystallite for current injected transverse to both the cylinder axis and the magnetic field. In this figure the open orbit was inclined at an angle $\theta = 72°$, an orientation in which current distortion effects are large. In strong fields the distortion regions persist for large distances, of order $(\omega_c\tau)R_0$, parallel to the magnetic field. At the same time, the effect of the magnetic field is to restrict the range of the current distortion in directions transverse to the magnetic field. In the infinite field limit there is no distortion of the current profile at all until the lines of current pass through the "shadow" of the singular crystallite. Once entering the shadow region, however, the current becomes compressed into thin sheets—shown as the dashed lines in Fig. 14—which flow nearly parallel to the magnetic field. The local power dissipation in these current sheets may be very great in strong fields and, in fact, it is this power density which is responsible for the transverse magnetoresistance induced by the crystallite; current "sucked" into the open-orbit channel from the outside medium contributes only a very small amount to the excess magnetoresistance. We thus reach the interesting conclusion that the magnetoresistance of polycrystalline copper does not arise directly from currents

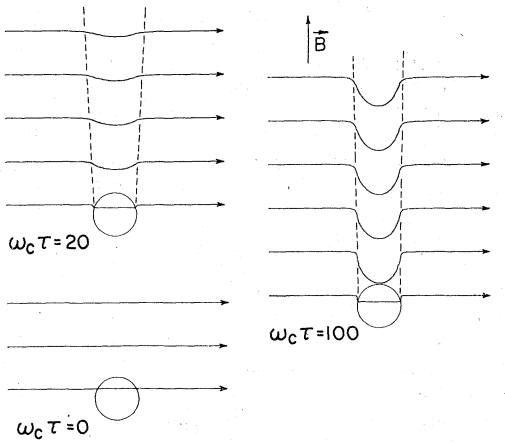

FIG. 14. Computer-generated distribution of the electric current flow pattern around an isolated cylindrical crystallite containing an open orbit. The open orbit lies in x-y plane and is inclined at an angle of 72° away from the direction of current injection.

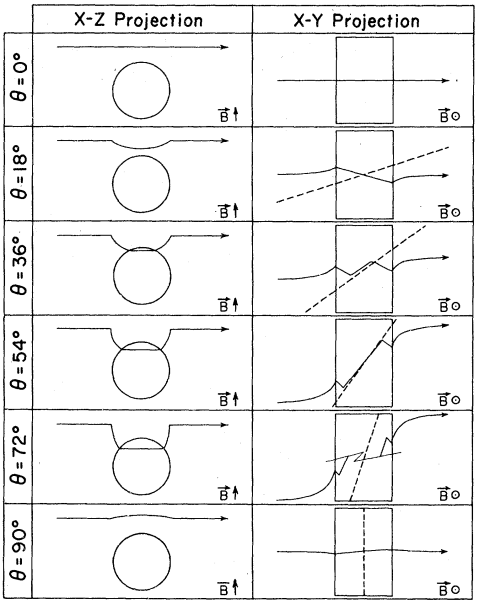

FIG. 15. Computer-generated distribution of the electric current flow pattern around an isolated cylindrical crystallite, illustrating the dependence on open-orbit orientation. All current profiles are for $\omega_c \tau = 100$, and θ is the angle between the open orbit and the direction of current injection.

flowing in open orbits. Instead, the magnetoresistance is a result of compressed current sheets flowing in closed-orbit crystallites, the effects of the open orbits being merely to introduce a highly localized perturbation into the potential field of the surrounding medium.

In Fig. 15, the dependence of the current distortion profile on the angle θ between the open-orbit direction and the direction of current injection is illustrated. Open orbits at $\theta = 0°$ and $\theta = 90°$ do not induce current distortion, while those oriented at $\theta = 76°$ have the largest effect. Also shown in the figure is a projection of typical current lines onto the x-y plane illustrating the "S"-shaped distortion which occurs as the current passes over the singular crystallite. This distortion pattern would obviously be modified by the presence of sample boundaries, although the modification would probably not be too great if the sample thickness was at least as large as the average crystallite diameter.

It must be noted that our model loses validity for metals of purity such that the electron mean free path is comparable to the crystallite size. For sufficiently long mean free paths the notion of associating a conductivity tensor with a single crystallite becomes tenuous. We have not attempted to estimate a crystallite diameter to mean-free-path ratio for the onset of this "size effect," and our data exhibit no systematic dependence upon such a ratio. Our model is intended primarily to explain qualitative behavior and may or may not be relevant to nonmacroscopic crystallites. We mention, however, that the long-range behavior of the current distortions is only slightly sensitive to changes in the "open orbit" conductivity tensor, and that other factors seem to have much greater influence upon the magnetoresistance over the range of sample purities and crystallite sizes studied here.

The magnetoresistance data of the polycrystalline flat plate samples in the $H_\perp$ configuration, shown in Figs. 7, 9, and 11, exhibited either a saturating or weak linear magnetoresistance in strong fields. Although we have not carried out detailed calculations of the current distribution in our samples for this field orientation, it is not difficult to estimate the transverse magnetoresistance for this case in the infinite-field limit. Following an argument suggested originally by Herring,[21] we note that the tangential component of the electric field at the boundary between a singular crystallite and the free-electron medium is given by

$$E_t = R_H B J_n + \rho J_t .$$

The subscripts t and n designate directions tangent and normal to the boundary of the singular crystallite, and R_H is the Hall coefficient of either the medium or the crystallite. Noting that R_H is discontinuous at the boundary while E_t and J_n are continuous, we conclude that the normal current $J_n \to 0$ in strong magnetic fields. This means that in the asymptotic field limit the lines of electric current will simply not cross over into the singular crystallites, and that the high-field magnetoresistance will saturate at a value approximately proportional to the fractional volume over which the current is excluded. This view appears to be consistent with our data, the sample-to-sample differences observed in our measurements being attributed primarily to statistical variations in crystallite size. In some samples we observed a slight linear term in the high-field magnetoresistance (see Fig. 9) although in all cases the Kohler slope $S_\perp$ was smaller than the slope $S_\parallel$ corresponding to the $H_\parallel$ orientation. As shown in Fig. 10, the value of $S_\perp$ increased with the parameter $\alpha = d/r_g$. Since α is a measure of the extent to which crystallites extended throughout the thickness of the sample, we conclude that the origin of this linear magnetoresistance is the same as that of the $H_\parallel$ configuration. For those crystallites not extending entirely through the sample, current shells tend to form in the region above and below the crystallite which enhance the magnetoresistance. This effect does

not occur for any crystallite larger than the sample thickness and the resistance simply saturates as current is excluded from such crystallites in strong fields.

The saturating longitudinal magnetoresistance observed in all our polycrystalline samples (see Fig. 12) is quite in accord with the predictions of the Lifshitz-Azbel-Kaganov theory. Open orbits have no effect on the longitudinal component of the conductivity tensor so that in all respects the longitudinal magnetoresistance of copper should be identical to that of a free-electron conductor. It is interesting to note, however, that the longitudinal magnetoresistance actually observed for the free-electron metals, e.g., potassium, in general has a linear field dependence. In this connection we note that inhomogeneities such as voids can induce a pronounced linear longitudinal magnetoresistance,[16,17] although, as mentioned previously, the role of such inhomogeneities in the simple metals has not yet been established. In our annealed copper samples, however, inhomogeneities did not appear to have any measurable effect on the longitudinal magnetoresistance.

To summarize, we believe our measurements have established that the high-field galvanomagnetic properties of polycrystalline copper are determined primarily by nonlinearities in the electric current distribution which occur as a natural result of a spatially inhomogeneous conductivity. The transverse magnetoresistance results from the concentration of current into narrow vertical sheets which propagate along the magnetic field lines for large distances above and below crystallites containing open or extended orbits. Our model calculations of the current profile around such crystallites are not capable of reproducing the explicit field dependence of the magnetoresistance since it is not practical to treat interaction effects among crystallites using this method. Nevertheless the general features of the distortion patterns are probably reasonable, particularly since the current shells are a consequence of the anisotropy of the free-electron medium and not of the particular conductivity of the singular crystallites. In other respects, we have found copper to have a conductivity tensor nearly perfectly specified by the theory of Lifshitz, Azbel, and Kaganov[41] and note that in this regard copper appears to be nearly unique among metals having uncomplicated Fermi surfaces.

ACKNOWLEDGMENTS

The authors wish to thank Professor A. B. Pippard for originally suggesting this topic, and Professor D. Stroud for several illuminating discussions. J. C. Garland wishes to acknowledge the kind hospitality of the Cavendish Laboratory during the early phases of this work, and J. B. Sampsell wishes to acknowledge the support of the Ohio State University for a University fellowship.

APPENDIX

In the general case we concern ourselves with a single cylindrical crystallite of resistivity

$$\vec{\vec{\rho}}=\begin{pmatrix}\rho_{11} & \rho_{12} & 0\\ \rho_{21} & \rho_{22} & 0\\ 0 & 0 & \rho_{33}\end{pmatrix} \tag{A1}$$

imbedded in an infinite medium of conductivity

$$\vec{\vec{\sigma}}=\sigma_0\begin{pmatrix}\gamma & \beta\gamma & 0\\ -\beta\gamma & \gamma & 0\\ 0 & 0 & 1\end{pmatrix}, \tag{A2}$$

where σ_0 is the zero-field conductivity, $\beta=\omega_c\tau$ is the effective magnetic field, $\gamma=(1+\beta^2)^{-1}$, and the magnetic field is oriented along the z axis. Following the method of Sampsell and Garland[16] we introduce a fictitious electric field $\vec{E}'(\vec{r}')$ and a scaled current density $\vec{J}'(\vec{r}')$ in the coordinate system $\vec{r}'=\vec{\vec{U}}\vec{r}$, where $\vec{\vec{U}}$ is given by

$$\vec{\vec{U}}=\begin{pmatrix}1 & 0 & 0\\ 0 & 1 & 0\\ 0 & 0 & \gamma^{1/2}\end{pmatrix}. \tag{A3}$$

A cylindrical crystallite of radius R_0 centered on the y' axis becomes an elliptical cylinder in this coordinate system where the convenient coordinates are

$$\begin{aligned}X'&=R_0\beta\gamma^{1/2}\cosh\mu\cos\theta,\\ Z'&=R_0\beta\gamma^{1/2}\sinh\mu\sin\theta.\end{aligned} \tag{A4}$$

Specifying the current far from the crystallite as $\vec{J}=J_{x0}\hat{x}$, we seek a solution for the potential outside the crystallite of the form

$$\begin{aligned}\Phi_e'(\vec{r}')&=(A\cos\theta+B\sin\theta)e^{-\mu}\\ &\quad-\beta(J_{x0}/\sigma_0)(y'+R_0\gamma^{1/2}\cosh\mu\cos\theta).\end{aligned} \tag{A5}$$

Inside the crystallite we follow the suggestion of Stachowiak and seek a solution of the form

$$\begin{aligned}\Phi_i'(\vec{r}')&=-E_{ix}'X'-E_{iy}'y'-E_{iz}'Z'\\ &=-(\rho_{11}J_{ix}'+\rho_{12}J_{iy}')R_0\beta\gamma\cosh\mu\cos\theta\\ &\quad-(\rho_{21}J_{ix}'+\rho_{22}J_{iy}')y'\gamma^{1/2}\\ &\quad-\rho_{33}J_{iz}'R_0\beta\sinh\mu\sin\theta.\end{aligned} \tag{A6}$$

Equating these potentials at the crystallite boundary, where by definition $\mu = \mu_0$, gives

$$A_e^{-\mu_0} = R_0[J_{x0}/\sigma_0 - \gamma^{1/2}(\rho_{11}J'_{ix} + \rho_{12}J'_{iy})] , \quad \text{(A7)}$$

$$B_e^{-\mu_0} = -\rho_{33}J'_{iz}R_0 , \quad \text{(A8)}$$

and

$$\gamma^{1/2}(\rho_{21}J'_{ix} + \rho_{22}J'_{iy}) = (\beta/\sigma_0)J_{x0} . \quad \text{(A9)}$$

Matching normal components of scaled currents at the boundary yields

$$A_e^{-\mu_0} = (R_0/\sigma_0)(J'_{ix} - J_{x0}/\gamma^{1/2}) \quad \text{(A10)}$$

and

$$B_e^{-\mu_0} = (R_0/\sigma_0\gamma^{1/2})J'_{iz} . \quad \text{(A11)}$$

Equations (A8) and (A11) require that $B = 0$, and combining Eqs. (A7), (A9), and (A10) allows us to solve for the remaining three unknowns J'_{ix}, J'_{iy}, and A:

$$J'_{ix} = \frac{1 - \beta(\rho_{12}/\rho_{22}) + 1/\gamma^{1/2}}{\gamma^{1/2}\rho_{11} - \gamma^{1/2}(\rho_{12}\rho_{21}/\rho_{22}) + 1/\sigma_0} \frac{J_{x0}}{\sigma_0} , \quad \text{(A12)}$$

$$J'_{iy} = (1/\gamma^{1/2}\rho_{22})[\beta(J_{x0}/\sigma_0) - \gamma^{1/2}\rho_{21}J'_{xi}] , \quad \text{(A13)}$$

$$A = e^{\mu_0}(R_0/\sigma_0)(J'_{ix} - J_{x0}/\gamma^{1/2}) . \quad \text{(A14)}$$

The value of μ_0 is given by $\sinh\mu_0 = \beta$.

The remainder of the solution is straightforward. The expressions for Φ'_e and Φ'_i are completely specified by the constants A, B, J'_{ix}, J'_{iy}, and J'_{iz}. Expressions for the current density and electric field in real space are found by transforming the scaled current density and fictitious field from the $\vec{r}'$ space. For example, the current density is given by

$$J_x(\mu,\theta) = \frac{\sigma_0\gamma^{1/2}}{R_0\beta} A \left(\frac{\sinh\mu\cos^2\theta - \cosh\mu\sin^2\theta}{\sinh^2\mu + \sin^2\theta}\right) e^{-\mu} + J_{0x} , \quad \text{(A15)}$$

$$J_y(\mu,\theta) = -\beta[J_x(\mu,\theta) - J_{x0}] , \quad \text{(A16)}$$

$$J_z(\mu,\theta) = \frac{\sigma_0}{R_0\beta} A \frac{\sin\theta\cos\theta}{\sinh^2\mu + \sin^2\theta} . \quad \text{(A17)}$$

†Research supported in part by NSF Grant No. DMR71-01794-A03.

*Present address: Department of Physics, Carnegie-Mellon University, Pittsburgh, Pa. 15213.

[1]H. J. de Wit, J. Appl. Phys. 43, 908 (1972).
[2]A. D. Pearson, J. Electrochem. Soc. 111, 753 (1964).
[3]R. W. Schmutzler and F. Hensel, J. Non-Cryst. Solids 8–10, 718 (1972).
[4]E. U. Franck and F. Hensel, Rev. Mod. Phys. 40, 697 (1968).
[5]U. Even and J. Jortner, Phys. Rev. Lett. 28, 31 (1972).
[6]B. Cabane and J. Friedel, J. Phys. (Paris) 32, 73 (1971).
[7]W. W. Warren, Jr., Phys. Rev. B 6, 2522 (1972).
[8]M. H. Cohen and J. C. Thompson, Adv. Phys. 17, 857 (1968).
[9]D. E. Schafer, F. Wadl, G. A. Thomas, J. P. Ferraris, and D. O. Cowan, Solid State Commun. 14, 347 (1974).
[10]For a summary of work pertaining to potassium see H. Taub, R. L. Schmidt, B. W. Maxfield, and R. Bowers, Phys. Rev. B 4, 1134 (1971); J. C. Garland *et al.*, *ibid.* 9, 1987 (1974); A. M. Simpson, J. Phys. F 3, 1471 (1973); F. W. Holroyd and W. R. Datars, Can. J. Phys. 53, 2517 (1975).
[11]J. C. Garland and R. Bowers, Phys. Rev. 188, 1121 (1969).
[12]R. J. Balcombe, Proc. R. Soc. A 275, 113 (1963).
[13]E. S. Borovik and V. G. Volotskaya, Zh. Eksp. Teor. Fiz. 48, 1554 (1965) [Sov. Phys.-JETP 21, 1041 (1965)].
[14]F. R. Fickett, Phys. Rev. B 3, 1941 (1971).
[15]W. Kesternich and H. Ollmaier, Phys. Lett. 36, 411 (1971).
[16]J. B. Sampsell and J. C. Garland, Phys. Rev. B 13, 583 (1976).
[17]D. Stroud and F. P. Pan, Phys. Rev. B 13, 1434 (1976).
[18]J. R. Klauder, W. A. Reed, G. F. Brennert, and J. E. Kunzler, Phys. Rev. 141, 592 (1966).
[19]P. Kapitza, Proc. R. Soc. A 123, 292 (1929).
[20]J. M. Ziman, Philos. Mag. 3, 1117 (1958).
[21]C. Herring, J. Appl. Phys. 31, 1939 (1960).
[22]D. A. G. Bruggeman, Ann. Phys. (Leipz.) 24, 636 (1935).
[23]R. Landauer, J. Appl. Phys. 23, 779 (1952).
[24]H. Stachowiak, Acta Phys. Pol. 23, 383 (1963); 24, 749 (1963); 25, 211 (1964); Bull. Acad. Pol. 15, 631 (1967); 15, 637 (1967); Physica (Utr.) 45, 481 (1970); Acta Phys. Pol. A 40, 849 (1971); Phys. Status Solidi A 20, 707 (1973).
[25]K. D. Schotte and D. Jacob, Phys. Status Solidi A 34, 593 (1976).
[26]D. Stroud, Phys. Rev. B 12, 3368 (1975).
[27]Yu. A. Dreizin and A. M. Dykhne, Zh. Eksp. Teor. Fiz. 63, 242 (1972) [Sov. Phys.-JETP 36, 127 (1973)].
[28]Yu. A. Dreizin and A. M. Dykhne, Pis'ma Zh. Eksp. Teor. Fiz. 14, 101 (1971) [JETP Lett. 14, 66 (1971)].
[29]F. R. Fickett, Ann. Report, Project 186 (1972), International Copper Research Assoc. (unpublished).
[30]F. R. Fickett, Proceedings of the Fourth International Conference on Magnet Technology, 1972, USAEC CONF-720908 (unpublished).
[31]C. M. Hurd and J. E. A. Alderson, Phys. Rev. B 4, 1088 (1971).
[32]J. de Launay, R. L. Dolecek, and R. F. Webber, J. Chem. Phys. Solids 11, 37 (1959).
[33]A. F. Clark and R. L. Powell, Phys. Rev. Lett. 21, 802 (1968).
[34]F. R. Fickett and A. F. Clark, J. Appl. Phys. 42, 217 (1971).
[35]T. G. Berlincourt, Phys. Rev. 112, 381 (1958).
[36]R. G. Chambers and B. K. Jones, Proc. R. Soc. A 270, 417 (1962).
[37]J. R. Klauder, W. A. Reed, G. F. Brennert, and J. E.

Kunzler, Phys. Rev. 141, 592 (1966).
[38]J. E. Alderson, T. Farrell, and C. M. Hurd, Phys. Rev. B 1, 3904 (1970).
[39]R. G. Chambers, Proc. R. Soc. A 238, 344 (1957).
[40]J. S. Dugdale and L. D. Firth, J. Phys. C 2, 1272 (1969).
[41]I. M. Lifshitz, M. I. Azbel, and M. I. Kaganov, Zh. Eksp. Teor. Fiz. 31, 63 (1956) [Sov. Phys.-JETP 4, 41 (1957)].